CFD Modeling and Simulation in Materials Processing 2016
Edited by: Laurentiu Nastac, Lifeng Zhang, Brian G. Thomas, Miaoyong Zhu, Andreas Ludwig, Adrian S. Sabau, Koulis Pericleous, and Hervé Combeau
TMS (The Minerals, Metals & Materials Society), 2016

MULTISCALE MODELING OF THE SOLIDIFICATION STRUCTURE EVOLUTION OF CONTINUOUSLY CAST STEEL BLOOMS AND SLABS

Laurentiu Nastac[1], Mikko Kärkkäinen [2], Pilvi Hietanen[2], Seppo Louhenkilpi[2]

[1]The University of Alabama, Department of Metallurgical and Materials Engineering,
Box 870202, Tuscaloosa, AL, 35487, USA
[2]Aalto University, Department of Materials Science and Engineering,
PO Box 16200, FI-00076, Espoo, Finland

Keywords. Multiscale Modeling; Continuous Casting; Blooms and Slabs; Low Alloying Steels; Solidification Structure; Columnar-to-Equiaxed Transition.

Abstract

An efficient multiscale mesoscopic modeling approach capable of accurately predicting the formation of the solidification structure during the continuous casting (CC) process was developed. The modeling approach consists of integrating a macroscopic model (TEMPSIMU3D+IDS) with a stochastic mesoscopic solidification structure model (SolMicro).
The integrated model can predict the evolution of the grain morphology and the columnar-to-equiaxed transition (CET) and is compared against experimental measurements for low-alloyed steel blooms and slabs, with dimensions of T312mm x W372 mm x L31m and T280 mm x W1962 mm x L31m, respectively. The validated model was then applied to determine the effects of superheat on the solidification structure of CC processed steel slabs.

Introduction

The objective of this work was to apply a transient multiscale modeling approach to get insights into the effect of key processing parameters on the solidification structure evolution during continuous casting (CC) processing of steel blooms and slabs. The modeling approach consists of integrating a transient macroscopic model with a mesoscopic solidification structure model. The integrated model can predict the solidification structure evolution of both columnar and equiaxed morphologies and the columnar-to-equiaxed transition (CET). The integrated model can assist thus in achieving better control of the casting solidification structure in these cast products. Another objective of this work determine the effects of superheat, casting rate and heat extraction rate on the solidification structure of CC processed steel blooms and slabs.
The capabilities of the model include the effects of process parameters, such as casting rate, mold cooling conditions and casting size on the casting structure at both the macroscopic and the microscopic levels. Thus, grain size, grain morphology (dendritic columnar or equiaxed), grain direction and CET can be predicted [1-5]. Other capabilities of the developed model include the capability to analyze the effects of melt transients, typically observed in the CC process.

L. Nastac et al. (Eds.), *CFD Modeling and Simulation in Materials Processing 2016*

A schematic of the CC process and the longitudinal cross-section of a CC-processed casting are illustrated in Figure 1. Figure 2 presents a schematic diagram showing the coupling between the transient computational fluid dynamics (CFD) code (**TEMPSIMU3D+IDS**) and the casting solidification structure code (**SolMicro**) [1-5].

IDS (InterDendritic Solidification) [7] uses a thermodynamic substitution model alongside a magnetic ordering model, mass balance equations and Fick's law to calculate the phase fractions and compositions of the solidifying steel as a function of temperature. The following phases are simulated: proeutectoid ferrite, cementite, pearlite, bainite, martensite and various non-metallic phases in the form of precipitates and inclusions. Complete solute mixing in the liquid is assumed. The model is capable of calculating the temperature-dependent material properties and phase composition evolution of both low and high-alloy steels.

TEMPSIMU3D [8] uses a parallel modified Gauss-Seidel-Newton-Rhapson solver to calculate the temperature field of a CC steel slab or bloom in 3D. The boundary conditions for the heat transfer simulation are defined using a physical model of the casting machine, taking into account the cooling effects of air-mist sprays, contact rolls and heat radiation, and accounting for the Leidenfrost effect. Currently, **TEMPSIMU** accounts for the effect of turbulent flow on heat transfer using a fitting coefficient. This coefficient modifies the thermal conductivity of steel as a function of the solid/liquid fraction. The value of this coefficient has been investigated using FLUENT simulations [9]. Together, **TEMPSIMU3D and IDS** can model solidification-kinetics, heat transfer and micro- and macro-segregation phenomena during casting and solidification of commercial cast products processed by the CC technology.

CC casting dimensions are shown in Table 1. Control parameters of the CC process, such as casting speed, mold cooling and secondary cooling conditions are typical for processing of steel blooms and slabs. Thermal properties of the materials used in the simulations are shown in Table 2 and Table 3. The data used in the **SolMicro** code are shown in Table 4. The nucleation parameters C_0, C_1, and C_2 are explained in Ref. [3], p. 160. G_{cr} is the critical temperature gradient for equiaxed nucleation and is used a criterion for calculation of CET (Ref. [3], p. 173).

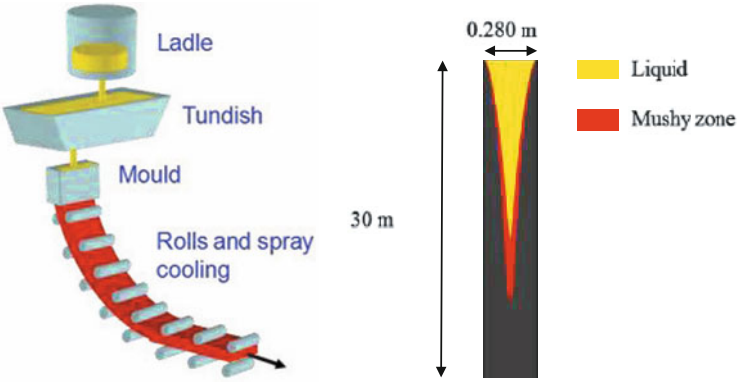

(a) (b)

Figure 1. (a) Schematic of the CC process [10] and (b) Longitudinal cross-section through a CC-processed slab (TEMPSIMU3D).

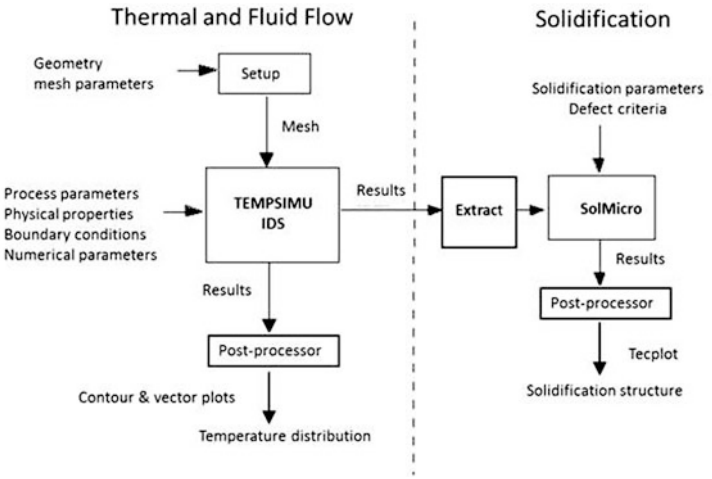

Figure 2. Coupling between **TEMPSIMU3D+IDS** simulation tools and **SolMicro** Stochastic Solidification Structure Simulator.

A special procedure was developed to compute and transfers all the transient information needed from the **TEMPSIMU3D+IDS** code to the **SolMicro** code including mushy-zone thermal gradients, cooling rates and solidification time.

As shown in Figure 2, the **TEMPSIMU3D+IDS** simulation code performs energy, momentum and solute transport computations to predict temperature, velocity and concentration distribution in the CC casting.

Then, from the transient temperature, concentration distributions computed by **TEMPSIMU+IDS** code, the **SolMicro** code computes the casting solidification microstructure evolution including grain morphology, grain size, and CET [6].

The **Extract** code computes and transfer all the information needed for the **SolMicro** simulator, including mushy-zone thermal gradients, cooling rates, and solidification time. The temperature history required by the **Extract** code is computed with the **TEMPSIMU** simulator. The additional solidification information required by **SolMicro** simulator is provided by **IDS** simulator.

Table 1. Boundary Conditions and Geometry for CC steel blooms and slabs

Model Conditions	Bloom	Slab A	Slab B
Casting width W[m]	0.372	1.974	1.962
Casting height, H[m]	0.312	0.279	0.279
Casting speed [m/min]	0.63	0.785	0.804
Mesh dimensions	47 x 40 x 613	50 x 20 x 617	50 x 20 x 617

Table 2. Thermal Properties of steel

Thermo-physical Property	Symbol	bloom	Slab A	Slab B
Density at solidus [kg m^{-3}]	ρ	7332	7318	7321
Thermal conductivity at solidus[W m^{-1} K^{-1}]	K	33.7	33.3	33.1
Liquidus temperature [C°]	T_L	1504	1505	1504
Solidus temperature [C°]	T_S	1453	1427	1422
Temperature of poured alloy [C°]	T_p	1559	1523	1548

Table 3. Enthalpy of steels (kJ/kg)

Temperature (C°)	Bloom	Slab A	Slab B
1600	1338	1329	1330
1500	1216	1206	1224
1400	930	922	923
1300	862	855	856
1200	795	788	789

Table 4. Data Used in Microstructure Modeling of steel

Solidification Kinetics Property	steel
Columnar nucleation parameters δN_c [nuclei m^{-2}]	$C_0 = 10^2$; $C_1 = 0$; $C_2 = 0$
Equiaxed nucleation parameters δN_e [nuclei m^{-3}]	$C_0 = 3.5 \times 10^5$; $C_1 = 3 \times 10^6$; $C_2 = 0$
Critical temperature gradient for CET, G_{cr} [K m^{-1}]	2000

Results and Discussion

The capability of the model to reconstruct CC bloom macrostructure was validated using measurements from a medium carbon Cr, Ni alloyed steel produced by OVAKO. Baumann (Sulfur) prints from the beginning, middle and end of a single heat were used to determine the location of the CET zone, as shown in figure 3. The modeled macrostructure for the top half of the CC bloom is shown in Figure 4. The model shows good agreement with the observed CET zone location.

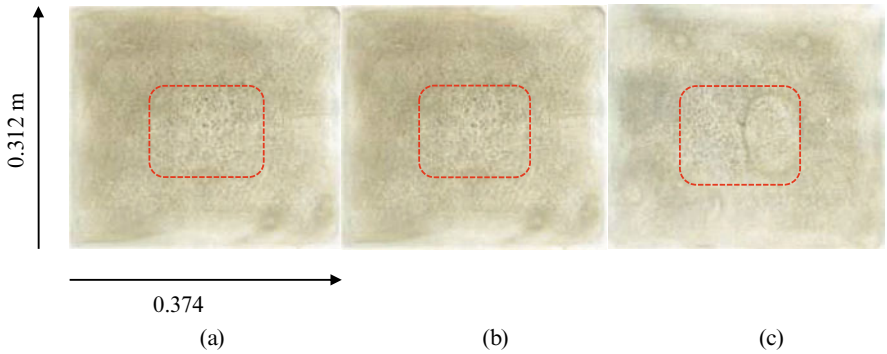

Figure 3. Baumann prints (Sulfur prints) of blooms at (a) start of cast, (b) center of cast, (c) end of cast highlighting the columnar-to-equiaxed transition.

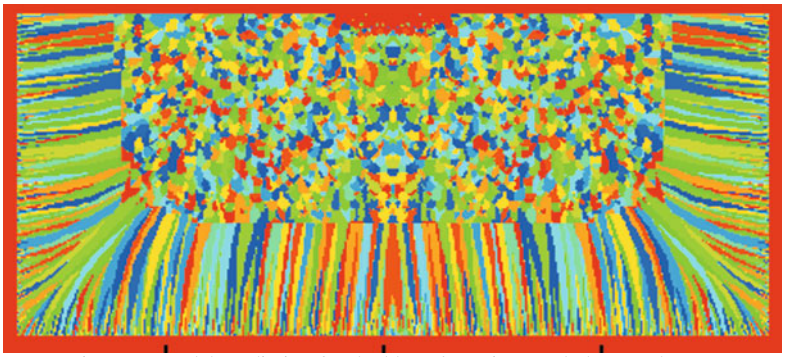

Figure 4. Model prediction for the bloom's grain morphology and CET.

The ability of the model to predict the slab macrostructure was validated using measurements from two slabs of a high-carbon medium-alloyed steel produced and analyzed by SSAB Europe Oy, Raahe. The slabs have similar composition but different values of superheat (45 K for slab B vs. 18 K for slab A). The ratio of different grain morphologies in the final macrostructures of the slabs is shown in figure 5.

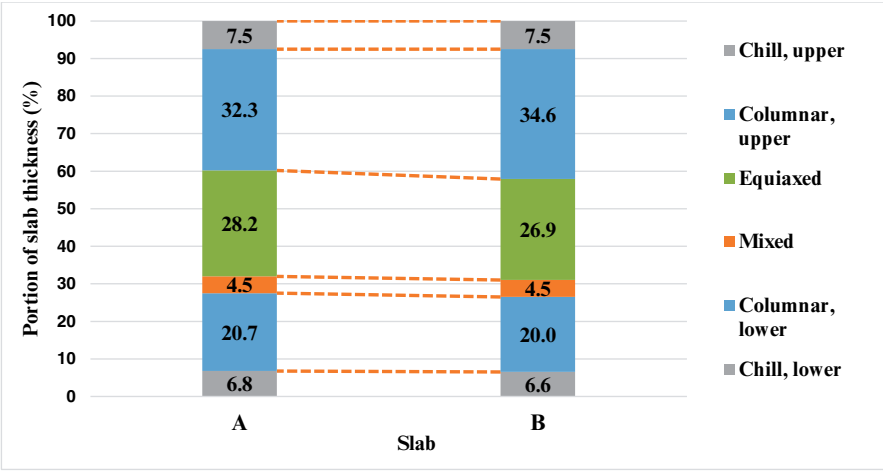

Figure 5. Experimental measurements of the grain morphology regions for slabs A and B.

The model predictions for the slabs A and B are shown in Figure 6. The measurements indicated 28.2% and 26.9% for the equiaxed grain region of the slab A and slab B, respectively. The model predicted an equiaxed-to-columnar ratio of 1:3 (~33% equiaxed grain region) for slab A and 1:3.3 for slab B (~30% equiaxed grain region). The predictions are in reasonable agreement with the experiments.

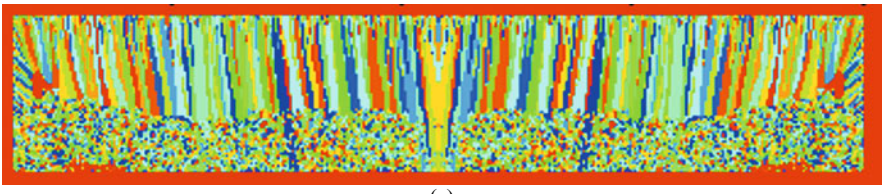

(a)

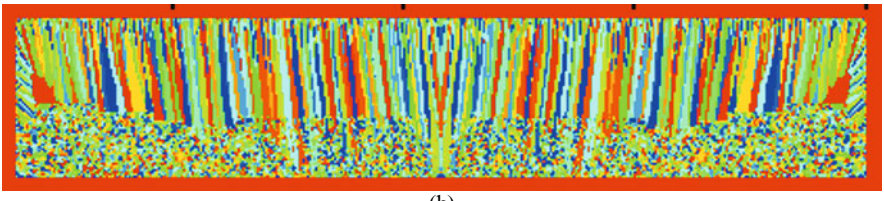

(b)

Figure 6. Model prediction for the slab's grain morphology and CET: (a) slab A and (b) slab B.

Conclusions and Future Work

An integrated multiscale transient modeling approach **TEMPSIMU3D+IDS** with **SolMicro**) was applied to simulate the solidification structure evolution during solidification of CC steel blooms and slabs. The integrated model was validated in terms of solidification structure against experimental data for CC processed steel blooms and slabs. The integrated modeling capability combined with prior production experience can be applied to determine the impact of casting conditions on the macrostructure behavior for different sizes of CC processed steel blooms and slabs and therefore it would potentially reduce the number of experimental trials needed in developing a new casting practice.
Future work will include additional model validation against experimental measurements in terms of grain size and CET for different steel alloys and for different sizes of blooms and slabs.

References

1. L. Nastac *et al.*, *Journal of Metals*, TMS, March 1998, pp. 30-35.
2. L. Nastac and A. Patel, Proc. of the Welding and Advanced Solidification Processes-MCWASP XI, Eds. C. Gandin and M. Bellet, TMS 2006, pp. 961-968.
3. L. Nastac, "Modeling and Simulation of Microstructure Evolution in Solidifying Alloys, Springer," Ney York, 2004 (ISBN 978-1-4020-7831-6).
4. L. Nastac, *Mat. Sc. and Tech.*, Vol. 28, No. 8, 2012, pp. 1006-1013.
5. L. Nastac, *Met Trans B*, Vol. 45B, 2014, pp. 44-50.
6. L. Nastac and D. M. Stefanescu, *Met Trans A*, Vol. 28A, 1997, pp. 1582-1587.
7. J. Miettinen, S. Louhenkilpi, H. Kytönen, and J. Laine, "IDS: Thermodynamic–kinetic–empirical tool for modelling of solidification, microstructure and material properties," *Math. Comput. Simul.,* Vol. 80, 2010, pp. 1536–50.
8. S. Louhenkilpi, M. Mäkinen, S. Vapalahti, T. Räisänen, and L. Laine, "3D steady state and transient simulation tools for heat transfer and solidification in continuous casting." *Mater. Sci. Eng. A,* Vol. 413-414, 2005**,** pp. 135–8.
9. P. Oksman, S. Yu, H. Kytönen, and S. Louhenkilpi, "The Effective Thermal Conductivity Method in Continuous Casting of Steel," *Acta Polytechnica Hungarica*, Vol. 11, No. 9, 2014, pp. 6-22.
10. S. Seetharaman, "*Treatise on Process Metallurgy, Volume 3: Industrial Processes*," Vol. 3. Newnes, 2013.